Xu, Zhengkai and Hyde, C.J. and Thompson, A. and Leach, R.K. and Maskery, I. and Tuck, C. and Clare, A.T. (2017) Defect evolution in laser powder bed fusion additive manufactured components during thermo-mechanical testing. In: Joint Special Interest Group meeting between euspen and ASPE Dimensional Accuracy and Surface Finish in Additive Manufacturing, 10-12 October 2017, Leuven, Belgium.

Joint Special Interest Group meeting between euspen and ASPE
Dimensional Accuracy and Surface Finish in Additive Manufacturing,
KU Leuven, BE, October 2017
www.euspen.eu

Defect evolution in laser powder bed fusion additive manufactured components during thermo-mechanical testing

Zhengkai Xu, C. J. Hyde, A. Thompson, R. K. Leach, I. Maskery, C. Tuck, A. T. Clare

Faculty of Engineering, The University of Nottingham, University Park, NG7 2RD, United Kingdom

zhengkai.xu@nottingham.ac.uk

Abstract
The mechanical performance of additively manufactured (AM) components remains an issue, limiting the implementation of AM technologies. In this work, a new method is presented, to examine the evolution of defects in an Inconel 718 two-bar test specimen, manufactured by laser powder bed fusion AM, during 'staged' thermo-mechanical testing. The test was interrupted at specific extensions of the specimen, and X-ray computed tomography measurements performed. This methodology has allowed, for the first time, the evolution of the defects in an AM specimen to be studied during a thermo-mechanical test. The number and size of the defects were found to increase with time as a result of the thermo-mechanical test conditions, and the location and evolution of these defects have been tracked. Defect tracking potentially allows for accurate prediction of failure positions, at the earliest possible stage of a thermo-mechanical test. Ultimately, when the ability to locate defects in this manner is coupled with manipulation of build parameters, laser powder bed fusion practitioners will be able to further optimise the manufacturing procedure in order to produce components of a higher structural integrity.

Creep, Two-bar specimen, X-ray computed tomography, Laser powder bed fusion, Mechanical testing, Nickel superalloys

1. Introduction

Laser powder-bed fusion (LPBF) additive manufacturing (AM) is a near-net-shape technique which provides a high design flexibility to components such as aero-engine turbine blades. However, few studies have considered thermo-mechanical properties such as creep, of specimens fabricated by such techniques. Rickenbacher et al. [1] investigated the creep performance of an LPBF fabricated In738LC specimen; the specimens' creep property was found to be anisotropic, and also slightly inferior to conventionally manufactured specimens. Pröbstle et al. [2] studied the creep properties of LPBF manufactured Inconel 718 specimens and found these specimens possess better creep performance than cast and wrought specimens, though fracture results were not included in their study. Conventionally, creep testing cannot provide direct evidence regarding defect evolution during a test, thus staged creep testing has been implemented. Through the use of X-ray computed tomography (XCT) at each stage, it is possible to study defect evolution in a non-destructive manner and continue mechanical testing. Babout et al. [3] designed an in-situ tomography system and applied it in room temperature tensile testing, obtaining seven scans at different stages of a tensile test. The propagation of defects in the specimen was successfully measured. Hangai et al. [4] applied a similar concept and compared the conditions of pores in an aluminium specimen pre and post fatigue testing of the specimen. This method gave direct evidence of defect development and a better understanding of the specimen behaviour during testing through determination of the fracture origin. The method can also be extended to other mechanical test types.

2. Methodology

In this study, a two-bar small specimen (TBS) was used to study creep (as shown in figure 1, in which the bold arrow indicates the building direction, L for left bar and R for right bar), and prove the practicality of the 'staged' testing technique. The TBS is a relatively small-sized specimen, designed by Hyde et al. [5], which can be used to obtain both creep strain rate and fracture life. Specimens of this geometry were built using a Renishaw AM250 LPBF system with commercial Inconel 718 powder provided by Renishaw PLC and milled to the specific dimensions shown. A specimen was tested with a tensile stress of 747.45 MPa at 650 ˚C and compared to a reference study by Sugahara et al. [6]. The test rig is shown in figure 2, where the TBS is mounted in the loading element and then encased in the heating element.

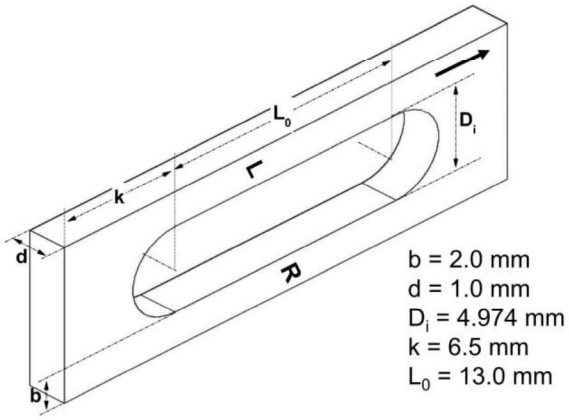

Figure 1. Dimensions of the TBS.

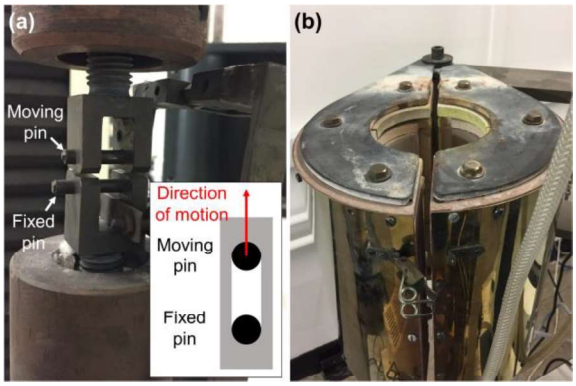

Figure 2. (a) Loading element and (b) heating element that make up the test rig.

A staged mechanical test was designed based on extension data obtained from preliminary experiments. The creep test was interrupted when the extension reached a certain distance, and the specimen was removed from the testing kit for XCT measurement. A Nikon MCT 225 was used to perform XCT measurements (settings: source voltage 225 kV, source current 44 µA, exposure 2000 ms and geometric magnification 20×, yielding a reconstructed voxel size of 10 µm ± 0.2 µm). The test strategy is shown in figure 3.

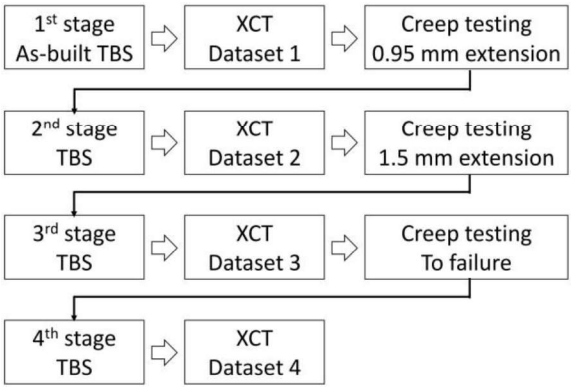

Figure 3. Staged creep testing strategy.

XCT image processing was performed using MATLAB [7] and ImageJ [8] to examine pores, based on thresholding via the ISO50 surface determination method [9]. The two-bar section (as shown in figure 4) was considered and measured.

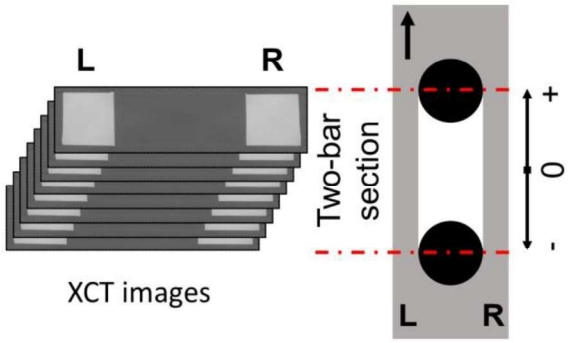

Figure 4. XCT images and the convention for the two-bar section.

3. Results and discussion

3.1. Porosity distribution in the TBS before mechanical testing

The right bar has higher porosity than the left (as shown in figure 5) and the porosity distribution has no regular pattern, which indicates that the pores in the AM manufactured parts are randomly distributed. The study made by Ziółkowski et al. [10] showed that the pore distribution was largely dependent on samples' building orientation. The section which has the highest porosity, i.e. peak 1, can be identified in the curve. The defects found at this position were considered at the first stage to be the likely cause of eventual fracture.

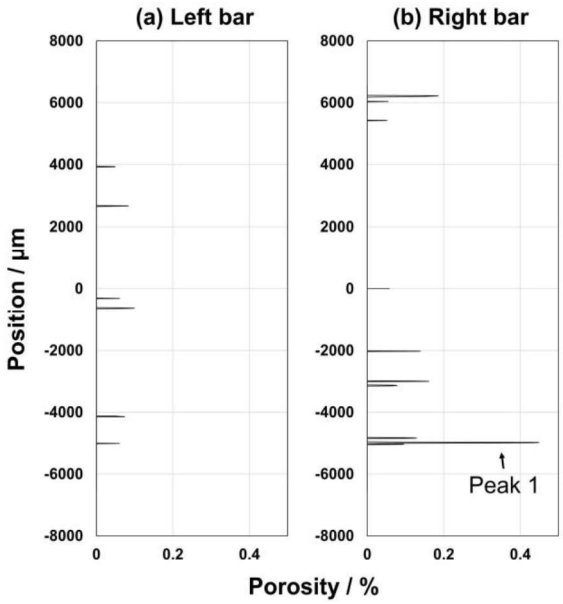

Figure 5. Porosity distribution in the TBS before testing.

3.2. Cross-sectional area changes

Figure 6 shows the decrease of the cross-sectional area in the two-bar section over the course of the creep test (necking). In this case, the most obvious reduction in the cross-sectional areas are located near the two ends. There is a 30% reduction of the cross-sectional area in the third stage when compared to the first stage and these positions represent likely potential fracture points. The negative end shown in figure 6 has an approximately 8% higher area reduction than the positive end. The negative end is more likely to cause the specimen's fracture.

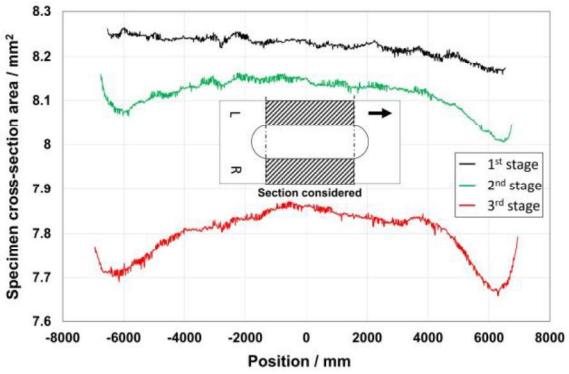

Figure 6. Cross-sectional area changes along the build direction.

3.3. Porosity distribution changes during mechanical testing

Figure 7 shows the porosity distribution change over time along the two bars of the specimen, with the greatest porosity increases being near the two ends. The specimen's fracture occurred in the negative end, as shown in figure 7. Peak 1 (same as the peak 1 in figure 5) has the highest porosity in the first stage (as-build condition). This peak disappeared in the fourth stage, indicating that the defects at this point resulted in the eventual fracture. This result agrees with the prediction made in section 3.1.

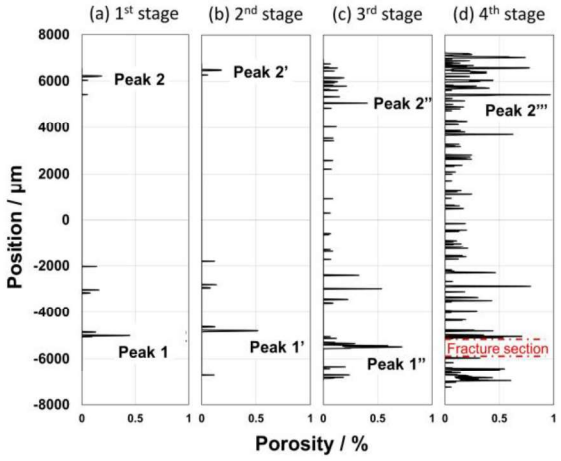

Figure 7. Porosity distribution change during testing.

3.4. Performance of the fracture section during the test

The reconstructed 3D model (as shown in figure 8) of the fracture section clearly indicates defects evolution. Pore 1 has an obvious ring shape in the first stage, which grew into a spherical pore during the test. Some newly developed pores are also observed in the third stage, which grew much faster than pore 1. These defects together cause the eventual fracture of the specimen. The small pore (pore 2 in figure 8) experienced almost no change during the testing.

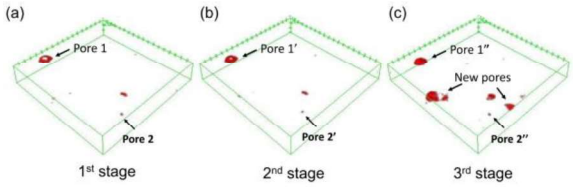

Figure 8. Reconstructed 3D model of the fracture section.

4. Conclusion

Defects in the as-build LPBF manufactured specimen are normally distributed randomly, and sections with the highest porosity are more likely lead to fracture. In the tested specimen, the most porous sections were found to be located at each end of the gauge sections, and the area of the respective cross-sections dropped significantly in these sections during testing. The evolution of pores in the fracture section involved the growth of existing pores in addition to the generation of the new pores. These mechanisms both contribute to specimen fracture.

The combination of the staged testing and XCT can be applied to estimate the potential fracture points and gain information of the subsequent specimen response, such as the pore evolution, in testing.

Acknowledgement

The authors would like to acknowledge the Engineering and Physical Sciences Research Council (EPSRC Grants EP/L017121/1, EP/M008983/1 and EP/L01534X/1) for funding this work. In addition, the authors would like to thank Alexander Jackson-Crisp for his invaluable technical contributions in machining specimens, Shane Maskill for facilitating the creep testing and to Renishaw Plc, process engineering team for providing Inconel 718 samples.

References

[1] Rickenbacher L, Etter T, Hövel S and Wegener K 2013 *Rapid Prototyping J.* **19** 282-29013
[2] Pröbstle M, Neumeier S, Hopfenmüller J, Freund L P, Niendorf T, Schwarze D and Göken M 2016 *Mat. Sci. Eng. A* **674** 299-307
[3] Babout L, Maire E, Buffière J Y and Fougères R 2001 *Acta Materialia* **49** 2055-2063
[4] Hangai Y, Kuwazuru O, Yano T, Utsunomiya T, Murata Y, Kitahara S, Bidhar S and Yoshikawa N 2010 *Mat. Trans.* **51** 1574-1580.
[5] Hyde T H, Ali B S M and Sun W 2013 *J. Eng. Mat. Tech.* **135** 041006-041006
[6] Sugahara T, Martinolli K, Reis D AP, Neto C de Moura, Couto A A, Neto F P and Barboza M J R 2012 *Defect and Diffusion Forum* **326-328** 509-514
[7] Marques O 2011 Practical Image and Video Processing Using MATLAB (Hoboken, New Jersey, Wiley) 368-370
[8] Schneider C A, Rasband W S and Eliceiri K W 2012 *Nat Meth* **9** 671-675
[9] Otsu N 1979 *IEEE Transactions on Systems, Man, and Cybernetics* **9** 62-66
[10] Ziółkowski G, Chlebus E, Szymczyk P and Kurzac J 2014 *Archives of Civil and Mechanical Engineering* **14** no. 4 608-614